Journal of Engineering and Applied Sciences 1(4): 323-328, 2006

Performance Characteristics of the Minkowski Curve Fractal Antenna

M. Ahmed, [1]Abdul-Letif, M.A.Z. Habeeb and [2]H.S. Jaafer
College of Science, Babylon University, Hilla, Iraq
[1]Minstry of Science and Technology, Baghdad, Iraq
[2]College of Science, Karbala University, Karbala, Iraq

Abstract: The performance properties of the Minkowski curve fractal antenna have been investigated and compared with the performance properties of the traditional straight-wire dipole. Numerical simulations were done using NEC4 which is moment-method based software. Results of radiation pattern, voltage standing wave ratio, input impedance, gain and half power beamwidth are provided. The results show that the self similarity properties of the fractal shapes are translated into its multiband behavior. It is concluded that the Minkowski curve fractal can be used to achieve miniaturization in antenna systems while maintening the radiation properties of the traditional straight-wire dipole. Thus this fractal antenna is likely to have a very promising future in portable device applications.

Key words: Fractal antennas, Minkowski curves, small antennas, iterated function system

INTRODUCTION

One of the prevailing trends in modern wireless mobile devices is a continuing decrease in physical size. In addition, as integration of multiple wireless technologies becomes possible, the wireless device will operate at multiple frequency bands. A reduction in physical size and multiband capability are thus important design requirements for antennas in future wireless devices. The geometry of the fractal antenna encourages its study both as a multiband solution[1-5] and also as a small physical size antenna[6-10]. First, because one should expect a self-similar antenna, which contains many copies of itself at several scales, to operate in a similar way at several wavelengths. That is, the antenna should keep similar radiation parameters through several bands. Second, because fractals are space filling contours, meaning electrically large features can be efficiently packed into small areas.

The first application of fractals to antenna design was thinned fractal linear and planar arrays[11-15], i.e., arranging the elements in a fractal pattern to reduce the number of elements in the array and obtain wideband arrays or multiband performance. Cohen[6] was the first to develop an antenna element using the concept of fractals. He demonstrated that the concept of fractal could be used to significantly reduce the antenna size without degenerating the performance. Puente *et al.*[4] demonstrated the multiband capability of fractals by studying the behavior of the Sierpinski monopole and dipole. The Sierpinski monopole displayed a similar behavior at several bands for both the input return loss and radiation pattern. Other fractals have also been explored to obtain small size and multiband antennas such as the Hilbert curve fractal[16], the Minkowski island fractal[9] and the Koch fractal[17]. The majority of this study will be focused upon the Minkowski curve fractal antenna and comparing its performance characteristics with those of the Half-Wavelength Dipole (HWD) antenna.

Analysis method and fractal geometry: Modeling and numerical simulations were done using NEC4 program. This program is based upon the Method of Moments (MoM) in which the electromagnetic interaction between wire segments can be analyzed. The MoM simulation technique incorporates periodic boundary conditions[18]. This allows for only one element of the periodic array to be simulated. When studying intricate elements such as fractals, this saves time and allows wide frequency sweeps. From the NEC4 software, the input impedance, radiation patterns, gain, Voltage Standing Wave Ratio (VSWR) and Half Power Beamwidth (HPBW) could be obtained.

The geometry of the fractal is important because the effective length of the fractal antenna can be increased while keeping the total special area relatively the same. As the number of iterations of the fractal increases, the effective length increases. A simple way to build most fractal structures is using the concept of Iterated Function System (IFS) algorithm, which is based upon a series of

Corresponding Author: M. Ahmed, College of Science, Babylon University, Hilla, Iraq

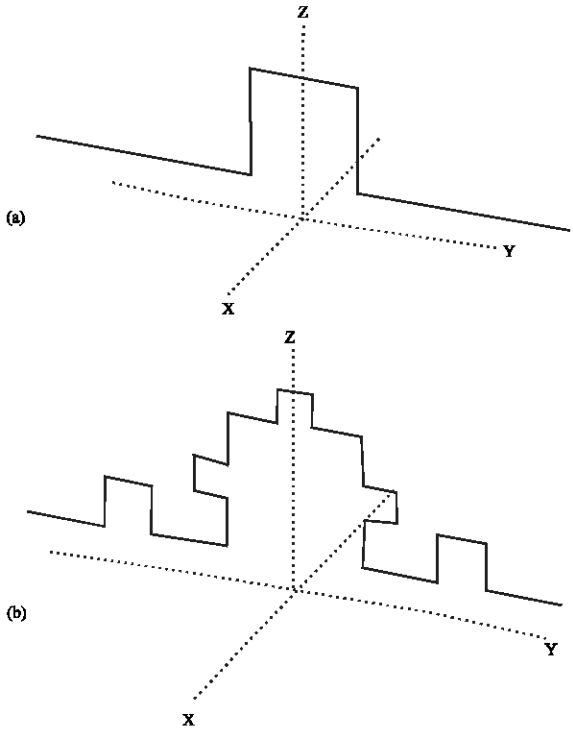

Fig.1: Geometry of the (a) minkowski curve fractal of one iteration (M1) and (b) minkowski curve fractal of two iterations (M2)

affine transformations[19]. An affine transformation in the plane (ω) can be written as:

$$\omega_q(x) = A_q x + t_q = \begin{bmatrix} r_{q1}\cos\theta_{q1} & -r_{q2}\sin\theta_{q2} \\ r_{q1}\sin\theta_{q1} & r_{q2}\cos\theta_{q2} \end{bmatrix} \begin{bmatrix} x_1 \\ x_2 \end{bmatrix} + \begin{bmatrix} t_{q1} \\ t_{q2} \end{bmatrix} \quad (1)$$

where x_1 and x_2 are the coordinates of point x. if r_{q1} r_{q2} r_q with $0<r_q<1$ and θ_{q1} θ_{q2} θ_q the IFS transformation is a contractive similarity (angles are preserved) where r_q is the scale factor and θ_q is the rotation angle. The column matrix t_q is just a translation on the plane. Applying these transformations, a Minkowski fractal of one Iteration (M1) and Minkowski fractal of two iterations (M2) are obtained as shown in Fig. 1. It is interesting to mention that M1 geometry exhibits a 24% reduction in the length from the HWD geometry, whereas the M2 geometry exhibits a 44% reduction in the length from the HWD geometry.

RESULTS AND DISCUSSION

Since all details of the radiation pattern follow from knowledge of the electric and magnetic dipole moments of the charge and current distribution in the antenna, these factors should be analyzed. To calculate the far-field of a HWD antenna of length L, it will be regarded that this antenna consists of a series of elemental short dipoles. The current distribution of any dipole with length L=2h (where h is the length arm of the dipole) placed on y-axis is given by[20]

$$I_{(y)} = I_m \sin(kh - ky) \quad \text{for} \quad y \geq 0 \quad (2)$$

$$I_{(y)} = I_m \sin(kh + ky) \quad \text{for} \quad y < 0 \quad (3)$$

where $k = 2\pi/\lambda$ and Im is the maximum value of the current which occurs at the center of the dipole (y=0). For the HWD where $h = \lambda/4$.

$$I_{(y)} = I_m \sin[k(\lambda/4) + k|y|] \quad (4)$$

where $|y| \leq \lambda/4$. The vector potential of y-directed line source is given by

$$A = \hat{y}\mu \frac{e^{-jkr}}{4\pi r} \int I_{(y)} e^{jky\cos\theta} dy \quad (5)$$

and since the electric field vector of y-directed source is given by

$$E_\theta = j\, w \sin\theta\, A\, \hat{\theta} \quad (6)$$

Then, one can obtain

$$E_\theta = j\, w\, \mu \sin\theta \frac{e^{-jkr}}{4\pi r} \int I_{(y)} e^{jky\cos\theta} dy \quad (7)$$

By substituting Eq. (4) in Eq. (7), the electric field vector becomes

$$E_\theta = j\, w\, \mu \frac{2I_m}{k} \frac{e^{-jkr}}{4\pi r} \frac{\cos\left(\frac{\pi}{2}\cos\theta\right)}{\sin\theta} \quad (8)$$

$$E_\theta = E_{max} \frac{\cos\left(\frac{\pi}{2}\cos\theta\right)}{\sin\theta} \quad (9)$$

Equation (9) gives the electric far field vector of the HWD antenna. The radiation patterns were generated at the resonant frequencies of the antennas. The computed patterns of the HWD, M1 and M2 antennas at the resonant frequency of 440 MHz are depicted in Fig. 2 and the corresponding three dimensional plots are displayed in Fig. 3. it is interesting to note that the radiation patterns

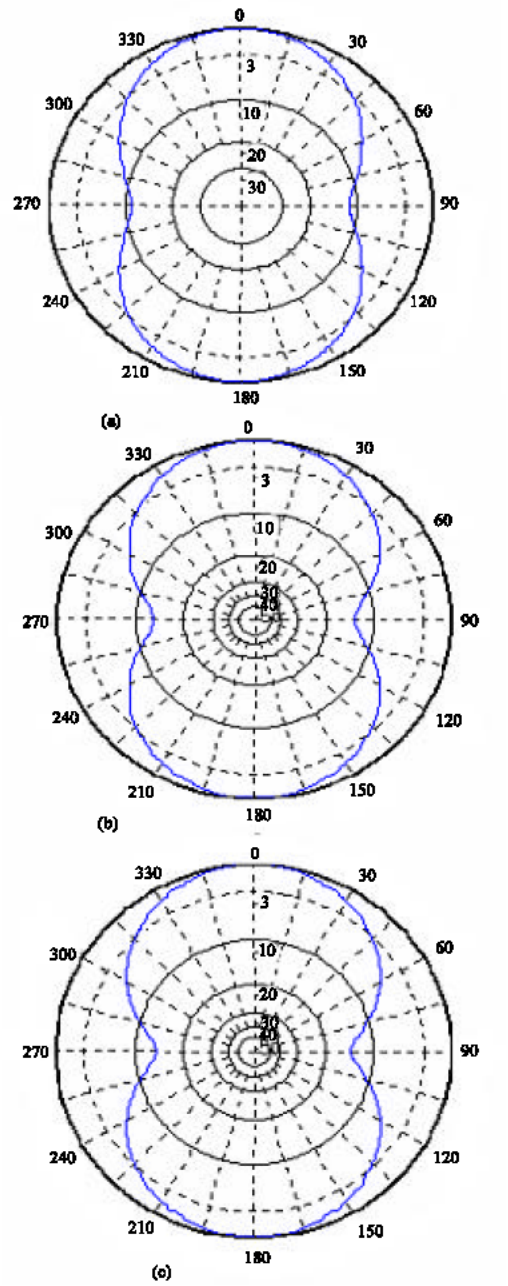

Fig.2: Radiation pattern at the resonant frequency of 440 MHz for the (a) half wavelength dipole (HWD) antenna, (b) M1 antenna and (c) M2 antenna

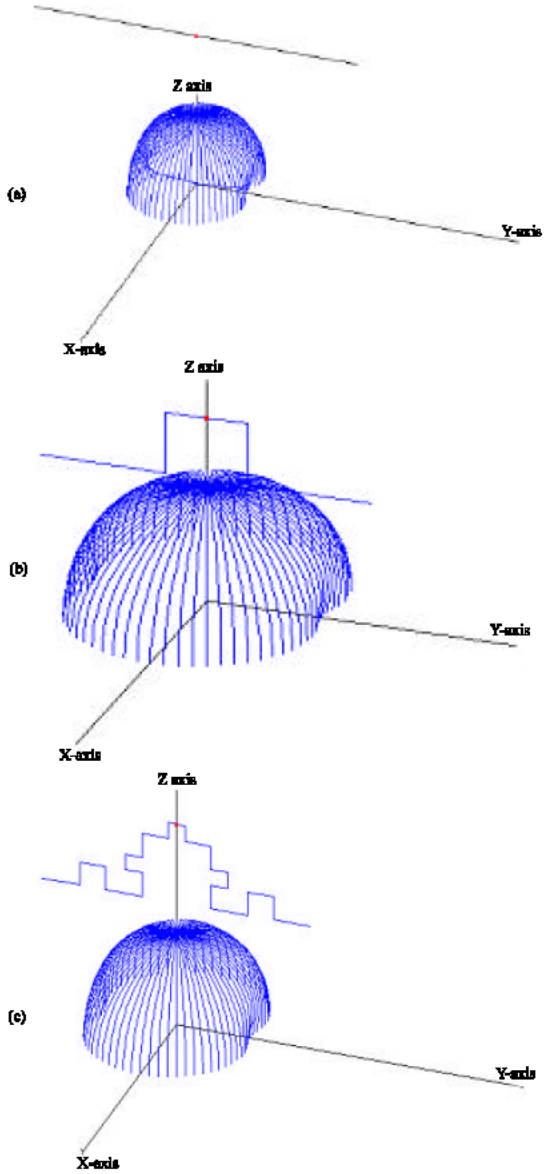

Fig. 3: Three dimensions plot of the radiation pattern at the resonant frequency of 440 MHz for the (a) HWD antenna, (b) M1 antenna and (c) M2 antenna

of the HWD, M1 and M2 antennas are similar. This indicates that these antennas exhibits virtually identical electromagnetic radiation behavior, independent of the difference in antenna size. What is also worth mentioning is the similarity between the other band's patterns of each the of M1 and M2 antennas. This is the proof for a truly multiband performance of the antenna. Over a large frequency span, the fractal antenna can have many different resonant frequencies. This is due to the coupling between the wires. As more contours and iterations of the fractal are added, the coupling becomes more complicated and different segments of the wire resonate at different frequencies.

As mentioned above, the radiation patterns were generated at the resonant frequencies of the antennas. The resonant frequencies could be estimated from the plot of the Voltage Standing Wave Ratio (VSWR) versus the frequency as shown in Fig. 4. It can be noted from this

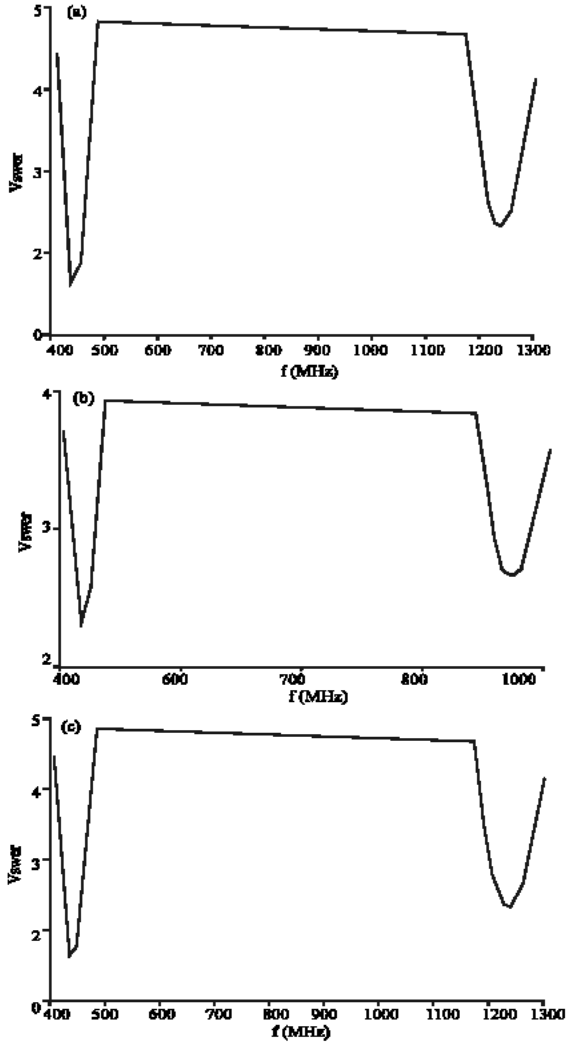

Fig.4: Voltage standing wave ration (VSWR)versus the frequency for the (a) HWD antenna, (b) M1 antenna and (c) M2 antenna

fiqure that each of the investigated antennas has resonant frequencies at 440 MHz and 1240 MHz in the frequency sweep of 400-1300 MHz. the VSWR values for a 50Ω transmission line of the HWD, M1 and M2 antennas are 1.4, 1.64 and 2.2, respectively.

There is one major parameter that is crucial to the design of efficient fractal antennas: That is the input impedance. The input impedance of a small linear dipole of length (ℓ) and wire radias (a) can be approximated by[21]

$$Z_{in} \cong 20\pi^2\left[\frac{\ell}{\lambda}\right]^2 - j\,120\frac{\left[\ln\left(\frac{\ell}{2a}\right)-1\right]}{\tan\left(\pi\frac{\ell}{\lambda}\right)} \qquad (10)$$

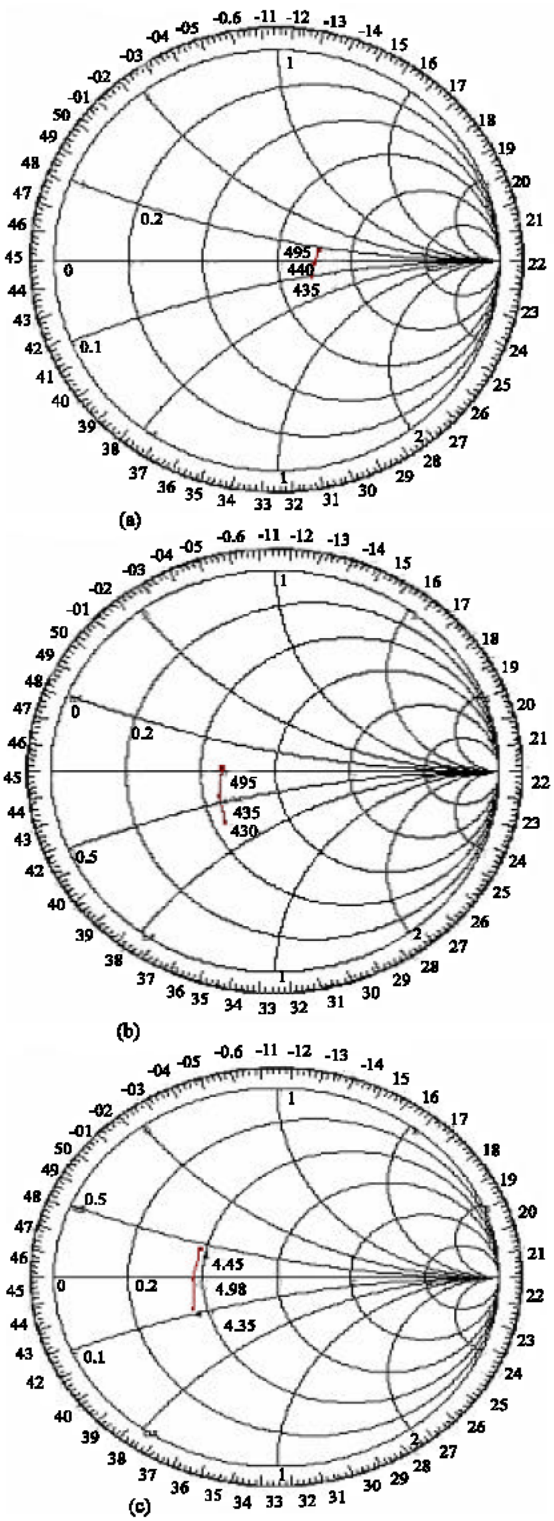

Fig. 5: Smith chart of the (a) HWD antenna, (b) M1 antenna and (c) M2 antenna

Table 1: Performance properties of the HWD, M1 and M2 antennas at 440 MHz

Parameter	HWD antenna	M1 antenna	M2 antenna
VSWR	1.4	1.64	2.2
Input Impedance (Ω)	70.19-j 1.1	30.95 + j 1.33	22.68-j 0.05
Gain (dBi)	2.11	2.01	1.91
HPBW	80o	88o	90o
Reduction of Length	0%	24%	44%

Or it can be measured, as it is done in the present work, by a rotation on the Smith chart to adjust the model of antenna to an RLC circuit. The Smith chart of the investigated antennas centered at the resonant frequency of 440 MHz were plotted using NEC4 software as shown in Fig. 5. it is noted from this figure that the matching of the Minkowski fractals are similar to the matching of the HWD antenna. The input impedances of the HWD, M1 and M2 antennas at the resonance frequency of 440 MHz are 70.19-j 1.1, 30.95 + j 1.33 and 22.68-j 0.05Ω, respectively. It can be shown that as the antenna iteration increases, the antenna has less input resistance, making it difficult to couple power to the antenna.

Other aspects of the antenna performance properties to consider are the gain and the Half Power Beamwidth (HPBW). The gains of the HWD, M1 and M2 antennas relative to an isotropic source, which radiates equally in all directions, were computed to be 2.11, 2.01 and 1.91 dB_i, respectively. It is noted that the fractal antenna has slightly less gain than the straight antenna. The HPBW was found to be 80o for the HWD antenna, 88o for the M1 antenna and 90o for the M2 antenna. It is obviously seen that the performance of the Minkowski fractals is better than that of the straight dipole in this property. A summary of the performance properties of the investigated antennas at the resonant frequency of 440 MHz is presented in Table 1.

The greatest advantage of the Minkowski fractal design is its compactness. This is highly significant for applications such as GSM cellular phones. Since the radiation pattern of the Minkowski fractal antenna is uniform and identical to that of a traditional HWD antenna, it can be used in nearly any type of wireless communications receiver. The superior HPBW performance of the Minkowski fractal antenna over the HWD antenna is another benefit of the design. Thus the Minkowski fractal antenna presents an excellent compact solution to the traditional straight-wire dipole.

CONCLUSION

Minkowski curve fractals can be used to achieve miniaturization in a ntenna systems while keeping an identical electromagnetic performance to the traditional straight-wire dipole. A size reduction of 24% was achieved using the M1 design over the straight HWD. A further size reduction of 44% was achieved using the M2 design over the straight HWD. It is concluded that the self similarity properties of the fractal shape are translated into its multiband behavior. Minkowski curve fractal antenna exhibits excellent performance at the resonant frequencies and has radiation properties nearly identical to that of the traditional straight wire dipole at that frequencies. Altogether, the fractal antenna is likely to have a very promising future in many applications such as portable communications devices.

REFERENCES

1. Gianvittorio, J.P. and Y. Rahmat-Sami, 2000. Fractal element antennas: a compilation of configurations with novel characteristics, antennas and propagation for wireless comm., IEEE Conf., pp: 129-132.
2. Puente, C., J. Romeu, R. Pous, X. Garcia and F. Benites, 1996. Fractal multiband antenna based on the Sierpinski gasket, Electron. Lett., pp: 1-2.
3. Romeu, J. and J. Soler, 2001. Generalized Sierpinski fractal multiband antenna, IEEE Trans. Antennas Propagat., pp: 1237-1239.
4. Puente, C., J. Romeu, R. Pous and A. Cardama, 1998. On the behavior of the Sierpinski multiband fractal antenna, IEEE Trans. Antennas Propagat., pp: 517-524.
5. Angnostou, D., C.G. Christodoulou and J.C. Lyke, 2002. Re-Configurable Array Antennas for Wideband Applications, IEEE Aerospace Conference.
6. Cohen, N., 1997. Fractal antenna applications in wireless telecommunications, Proceeding of Electronics Industries Forum of New England, pp: 43-49.
7. Puente, C., J. Romeu, R. Pous, J. Ramis and A. Hijazo, 1998. Small but long Koch fractal monopole, Electronics letters, pp: 9-10.
8. Puente, C., J. Romeu and A. Cardama, 2000. The Koch monopole: A small fractal antenna, IEEE Trans. Antennas Propagat. pp: 1773-1781.
9. Gianvittorio, J.P. and Y. Rahmat-Sami, 2002. Fractal antennas: A novel antenna miniaturization technique and applications, IEEE Antennas and Propagation Magazine, pp: 20-36.
10. Gianvittorio, J.P. Fractals, 2003. MEMS and FSS electromagnetic Devices: Miniaturization and multiple resonances, PhD Thesis, University of California, Los Angeles.

11. Kim, Y. and D.L. Jaggard, 1986. The fractal random arrays Proc. IEEE, pp: 1278-1280.
12. Werner, D.H. and P.L. Werner, 1996. Frequency independent features of self-similar fractal antennas, Radio Sci., pp: 1331-1343.
13. Puente, C. and R. Pous, 1996. Fractal design of multiband and low side-lobe arrays, IEEE Trans. Antennas Propagat., pp: 730-739.
14. Werner, D.H. and R.L. Haupt, 1997. Fractal constructions of linear and planar arrays, Digest of IEEE AP-S/URSI Intl. Symposium, pp: 1968-1971.
15. Jaggard, D.L. and A.D. Jaggard, 1998. Contor ring arrays, Digest of IEEE AP-S/URSI Il. Symposium, pp: 866-869.
16. Vinoy, K.J., K.A. Jose, V.K. Varadan and V.V. Varadan, Hilbert curve fractal antenna: A small resonant antenna for VHF/UHF applications, Microwave and Optical Technology Lett., 4: 215-219.
17. Best, S.R., 2003. On the performance properties of Koch fractal and other bent wire monopoles, IEEE Trans. Antennas Propagat., pp: 1292-1300.
18. Barlevy, A.S. and Y. Rahmat-Sami, 2001. Characterization of electromagnetic band-gaps composed of multiple periodic tripods with interconnecting vias: Concept, analysis and design, IEEE Trans. Antennas Propagat.
19. Werner, D.H. and S. Ganguly, 2003. An overview of fractal antenna engineering research, IEEE Antennas and propagation Magazine, pp: 38-56.
20. Stutzman, W.I. and G.A. Thiele, 1998. Antenna theory and design, New York, John Wiely and Sons.
21. Balanis, C.A., 1997. Antenna Theory: Analysis and Design, 2nd Ed., New York, John Wiley and Sons.